JOURNAL OF GEOPHYSICAL RESEARCH, VOL. 105, NO. D9, PAGES 11,739–11,752, MAY 16, 2000

Cloud processing of continental aerosol particles: Experimental investigations for different drop sizes

Martina Krämer
Institut für Stratosphärische Chemie (ICG-1), Forschungszentrum Jülich, Jülich, Germany

Norbert Beltz[1] and Dieter Schell[2]
Zentrum für Umweltforschung, Universität Frankfurt, Germany

Lothar Schütz, Cornelia Sprengard-Eichel,[3] and Sabine Wurzler
Institut für Physik der Atmosphäre, Universität Mainz, Mainz, Germany

Abstract. Atmospheric aerosol particles are activated and grow into drops during the formation of a cloud. Subsequently, they are delivered from the dissipating cloud drops back to the atmosphere. During the cloud lifetime, the drops scavenge water-soluble trace gases, leading to an increase in size and solubility of the particles emerging from the evaporating cloud drops. This processing of aerosol particles by clouds has an influence on the microphysics of the following cloud and its probability to rain as well as on the cooling effect of the direct and indirect aerosol forcing of climate. To measure the cycling history (particle activation and gas scavenging in drops followed by processing of the activated particles followed by emerging processed particles) of continental aerosol particles passing through cloud drops of different sizes, a new method is developed and applied during three field experiments carried out on the Mount Kleiner Feldberg/Ts., Germany, in 1990, 1993, and 1995. The typical droplet spectra of most of the observed stratus clouds is weakly bimodal, with mode 1 at drop sizes between 3 and 5 μm and mode 2 between 5 and 10 μm radius. Cloud drops in this overall size range are subject to growth only by condensation, while coalescence can be neglected. Therefore the observed processing is related solely to gas scavenging and in-cloud chemical reactions. We found that the processing of particles is different for the two modes of the cloud drop size spectrum: Small activated particles mostly grow to the small drops of mode 1, while larger particles can grow further to the larger drops of mode 2. Likewise, the mass of scavenged gas is, on average, lower for the small than for the larger drops. Vice versa, the ratio of scavenged gas to particle mass, the parameter quantifying the particle processing, is, on average, found to be higher in the small drop mode containing the smaller particles. The reason is that the degree of processing is mainly inversely linked to the mass of the activated particles. Therefore the strongest modification of particles takes place in smaller drops and affects mainly the smaller activated particles ($r_{ap} \leq 0.1$ μm). Their radii can increase by up to a factor of 3 and, consequently, their nucleation as well as radiative properties change significantly. The consequence for the aerosol climate forcing is that the cooling can be, to an unknown extent, intensified with increasing atmospheric amount of water-soluble trace gases such as HNO_3, NH_3, and SO_2, counteracting the warming effect of the greenhouse gases.

1. Introduction

Atmospheric aerosol particles are activated and grow into drops during the formation of a cloud. Subsequently, they are delivered from the dissipating cloud drops back to the atmosphere. During the cloud lifetime, the drops scavenge water-soluble trace gases and, if the drops are large enough, coalescence of droplets will occur. Both processes lead to an increase in size of the particles emerging from the evaporating cloud drops (if no outgassing occurs during evaporation), while the former (chemical processing) will also increase the soluble fraction of those particles. This processing of aerosol particles by clouds is a focus of recent research because it forces the Earth's climate in two ways [e.g., *Charlson et al.*, 1992; *Schwartz et al.*, 1995], both having a cooling effect on the atmosphere: (1) directly, because processing tends to increase the particles size and soluble fraction and thus to change their growth rate in dependence of the relative humidity of the ambient air; After *Pilinis et al.* [1995] and *Nemesure et al.* [1995], this is the major effect influencing the scattering of the incoming solar radiation by particles; (2) indirectly, as during the formation of a new cloud in the same air mass, the processed particles serve as condensation nuclei which activate at lower supersatura-

[1]Now at Lahmeyer GmbH, Bad Viebel, Germany.
[2]Now at enviscope GmbH, Frankfurt/Main, Germany.
[3]Now at Procter & Gamble GmbH, Schwalbach, Germany.

Paper number 1999JD901061.
0148-0227/00/1999JD901061$09.00

tions than before [*Choularton et al.*, 1996] because their size and soluble fraction have increased. This influences the drop size spectrum of the new cloud in the sense that for the same supersaturation a cloud with more but smaller drops will develop. Subsequently, the cloud lifetime is longer, and the albedo has increased, which means the cloud is "whiter" [e.g., *Slingo*, 1990; *Bower et al.*, 1997]. Furthermore, the change in the drop spectrum influences the probability of rain formation [*Bower and Choularton*, 1993; *Eichel et al.*, 1996] which ultimately impacts on the atmospheric lifetime of the aerosol particles.

Up to now, the cycling of aerosol particles through clouds is not completely understood. It is a very complex process in space and time, influenced by many factors. To obtain the full picture of the modification of the aerosol particle size spectrum by passage through a cloud, not only the particle scavenging mechanisms and the collision-coalescence of drops but also the gas uptake by the resulting cloud drop population and subsequent liquid phase reactions must be known. Moreover, upon cloud drop evaporation the desorption of gases should be considered.

Many ground-based and airborne field experiments (for example, in Europe: 1989 in the Po Valley, Italy [*Heintzenberg*, 1992], 1990 on the Mount Kleiner Feldberg, Germany [*Fuzzi*, 1994], 1993 at Great Dun Fell, England [*Fuzzi*, 1997], and 1993 above southern Bavaria, Germany [*Meischner et al.*, 1993] as well as model studies [e.g., *Bott*, 1995; *Bott et al.*, 1996; *Bower and Choularton*, 1993; *Bower et al.*, 1997; *Eichel et al.*, 1996; *Kulmala et al.*, 1993; *Wurzler et al.*, 1994, 1995, 1997; *Korhonen et al.*, 1996; *Kulmala et al.*, 1998] have been carried out in the last decade to study the processes listed above. However, there is still a lack of information, on the one hand because of the limits in the resolution in time and space of the measured parameters and, subsequently, of the input data for the models. Additionally, not all required parameters can be measured. On the other hand, also the models are subject to limitations in the sense that they cannot include all physical and chemical processes in space and time. Moreover, investigations of cloud processing should be carried out in different regions (e.g., urban, continental, marine) because each zone has its typical physicochemical characteristics of the aerosol particles, concentrations of different gaseous species, and other atmospheric conditions.

In the present study we developed a new method to determine experimentally the full chemical cycling history (particle activation and gas scavenging in drops followed by processing of the activated particles followed by emerging processed particles) of aerosol particles passing through cloud drops of different sizes. The advantage of the method is that from only a few measurements in bulk cloud water it is, with the knowledge of some key parameters and a meaningful data analysis, possible to conclude backward to the activated particles and forward to the processed particles. Prerequisite for the key parameters is a measuring site well characterized in terms of a large database of aerosol and cloud physics and chemistry. The method is applied during three field campaigns, performed on the continental site Mount Kleiner Feldberg/Ts., Germany, in 1990, 1993, and 1995 (FELDEX).

The basic principle of the method is as follows (a detailed description of the various instruments, sampling and analysis methods, as well as data processing is given in section 2 (for symbols and acronyms see Table 1)): Aerosol particles in cloud-free air are sampled and their mean soluble and insoluble fraction (AP_{sol}, AP_{ins}) is determined. When a cloud is formed in the same air mass, bulk cloud water in different drop size classes is sampled and analyzed for the amount of soluble and insoluble mass (C_{sol}, C_{ins}). Mass accretion of soluble substances due to gas scavenging increases the amount of soluble material in the cloud water compared to the originally activated particles, while the insoluble material remains constant because particle activation is its only pathway into the cloud drops. By knowing the "activated" (AP_{sol}/AP_{ins}) and the "processed" (C_{sol}/C_{ins}) ratios of soluble to insoluble material, the cloud water mass concentration resulting from the gas scavenged by the cloud drops (C_{gas}) can be determined. Subsequently, the cloud water mass concentration originating from the activated particles (C_{ap}) can be calculated. This procedure is applicable, if the ratio AP_{sol}/AP_{ins} measured in cloud-free air is also representative for those particles activated during cloud formation, which is shown in section 2.2.2.

Additionally, detailed cloud drop spectra are measured in cloudy periods. From these measurements, functional relationships ("calibration functions") are derived, relating, for each bulk cloud water sample, the liquid water mass of the sampled drops (LWC^{samp}) to their number (N_{drop}^{samp}) and mean size (r_{drop}). With this information the parameters measured in bulk cloud water can be related to cloud drops of a certain size: the mean scavenged gas mass per drop (M_{gas}) and the mean mass and size of activated particles (M_{ap}, r_{ap}).

If the cloud drops evaporate without outgassing (and our measurements show that this does not play an important role for our samples; see section 2.6), the "processed" ratio of soluble to insoluble mass is preserved in the processed particles that emerge from the different size cloud drops. Therefore the growth factor (gf) of the activated particles and size of the processed particles (r_{cp}) can also be determined from the measurements in cloud water.

Summarizing, application of the new method gives insight into the processes of size differentiated particle activation to drops of different size, subsequent scavenging of trace gases in dependence on drop size, and therefore the size differentiated particle processing in drops of various sizes. The aim of this study is to introduce the new method and present results for continental particles cycling through stratus clouds during the field experiments on Mount Kleiner Feldberg/Ts., Germany, in 1990, 1993, and 1995.

Here we would like to note that from these measurements, also information on the alteration of the solubility of particles by cloud processing can be achieved [*Krämer*, 1998]. Additional determination of the ion composition of the bulk cloud water samples allow specification of the main ions entering the drops of different size and therefore are responsible for the particle growth and chemical composition of the processed particles (M. Krämer et al., submitted manuscript, 1999).

2. Method: Instruments, Sample Analysis, and Data Processing

First, the experiments, the instrumentation, and the microphysics of the clouds (i.e., the cloud drop size spectra dN_d/dr_d, measured with FSSP) observed at the measuring site are presented (section 2.1). We then specify in detail the above described new method to obtain extended information about aerosol processing in cloud drops on the basis of only few measurements in bulk cloud water (sections 2.2–2.6). The closing section 2.7 attends to uncertainties (while in each section, the respective errors will be treated) and gives a final summary

Table 1. Symbols and Acronyms

Parameter	Unit	Meaning	Derivation
AP_{ins}	%	mean insoluble fraction of bulk aerosol particles	measured by SoFA
AP_{sol}	%	mean soluble fraction of bulk aerosol particles	measured by SoFA
AP_{sol}^{cp}	%	mean soluble mass fraction of processed particles	measured by SoFA
$Eff(r_d)_{(RC,TFI)}$		efficiency curves of the cloud water collectors	
$LWC_{(FSSP)}^{samp}$	mg/m^3	sampled liquid water content (from FSSP)	$\int \left(\frac{dM_{drop}}{dr_d} \cdot Eff(r_d)\right) dr_d$
$LWC_{(TFI,RC)}^{samp}$	mg/m^3	sampled liquid water content (from RC, TFI)	from sampled cloud water
M_{drop}, M_p	ng	mass of drops, particles	
N_d	cm^{-3}	number of drops	
$N_{drop,i}$	cm^{-3}	total drop number of sample i (from FSSP)	$\int \left(\frac{dN_{drop,i}}{dr_d}\right) dr_d$
$N_{drop,i}^{samp}$	cm^{-3}	sampled drop number of sample i (from FSSP)	$\int \left(\frac{dN_{drop,i}}{dr_d} \cdot Eff(r_d)\right) dr_d$
N_{drop}^{samp}	cm^{-3}	sampled drop number (calculated from calibration curves)	$f(LWC^{samp})$
r_d, r_p	μm	radius of drops, particles	
r_{drop}	μm	mean radius of drops of one sample	$\left(\frac{3}{4\pi} \cdot \frac{LWC^{samp}}{N_{drop}^{samp}}\right)^{1/3}$
Λ_{eqH^+}	$\frac{\mu Scm^{-1}}{\mu eqL^{-1}}$	equivalent conductivity of H^+	0.35
$\bar{\Lambda}_m$	$\frac{\mu Scm^{-1}}{mgL^{-1}}$	mean mass conductivity of all other ions	1.88
pH		acidity of cloudwater	
H^+	$\mu eq/L$	equivalent conc. in cloudwater	$10^{-pH} \times 10^6$
σ	$\mu S\ cm^{-1}$	electric conductivity	
C_{sol}	mg/L	cloudwater conc. of soluble mass	$\frac{\sigma - [H^+]\Lambda_{eqH^+}}{\bar{\Lambda}_m}$
C_{ins}	mg/L	cloudwater conc. of insoluble mass	$\int \left(\frac{dM_p}{dr_p}\right) dr_p$
C_{tot}	mg/L	cloudwater total mass conc.	$C_{sol} + C_{ins} = C_{ap} + C_{gas}$
C_{gas}	mg/L	cloudwater conc. from gas scav.	$C_{sol} - \left(\frac{AP_{sol}}{AP_{ins}} \cdot C_{ins}\right)$
C_{ap}	mg/L	cloudwater conc. from activated particles	$C_{tot} - C_{gas}$
M_{tot}	ng/drop	mean total mass per drop	$M_{tot} = M_{ap} + M_{gas}$
M_{gas}	ng/drop	mean gas mass per drop	C_{gas}/N_{drop}^{samp}
M_{ap}	ng/drop	mean activated particle mass per drop	C_{ap}/N_{drop}^{samp}
M_{ap}^{gas}		scavenging ratio: gas/particle mass per drop	M_{gas}/M_{ap}
M_{sol}^{cloud}	%	mean soluble mass fraction in cloud drops	
r_{ap}	μm	mean radius of activated particles	$\left(\frac{3}{4\pi\rho_{ap}} M_{ap}\right)^{1/3}$
ρ_{ap}	gcm^{-3}	mean particle density	1.5
r_{cp}	μm	mean radius of processed particles	$\left(\frac{3}{4\pi\rho_{ap}} M_{tot}\right)^{1/3}$
gf		particle growth factor	r_{cp}/r_{ap}

Instrument	Meaning	Measured Parameter
SoFA	soluble fraction of aerosols—analyzer	AP_{sol}, AP_{ins}
FSSP	forward scattering spectrometer probe	cloud drop size spectrum, $\frac{dN_{drop}}{dr_d}$
RC	rotating arm collector	bulk cloudwater, $r_d > 7\ \mu m$
TFI	two-stage fogwater impactor	bulk cloudwater
TA93	first stage of TFI in 1993	$r_d > 6.5\ \mu m$
TA95	first stage of TFI in 1995	$r_d > 5\ \mu m$
TB	second stage of TFI	$2.5 < r_d < 5\ \mu m$

Parameters are listed in the order of appearance in the text.

of the quality of the method. To make the method easier to understand, a summarizing overview of the measured and calculated parameters is given in the Appendix. The parameters to be measured in each bulk cloud water sample taken with the samplers TFI(TA,TB) and RC, i.e., LWC^{samp}, pH, σ, C_{ins}, are given in the overview. The key statements central for the method in sections A1, A2, A3, and A5 of the overview are as follows: (1) the mean soluble and insoluble fraction of aerosol particles in cloud-free air is constant (AP_{sol}/AP_{ins} = const.) and representative for the particles activated during cloud for-

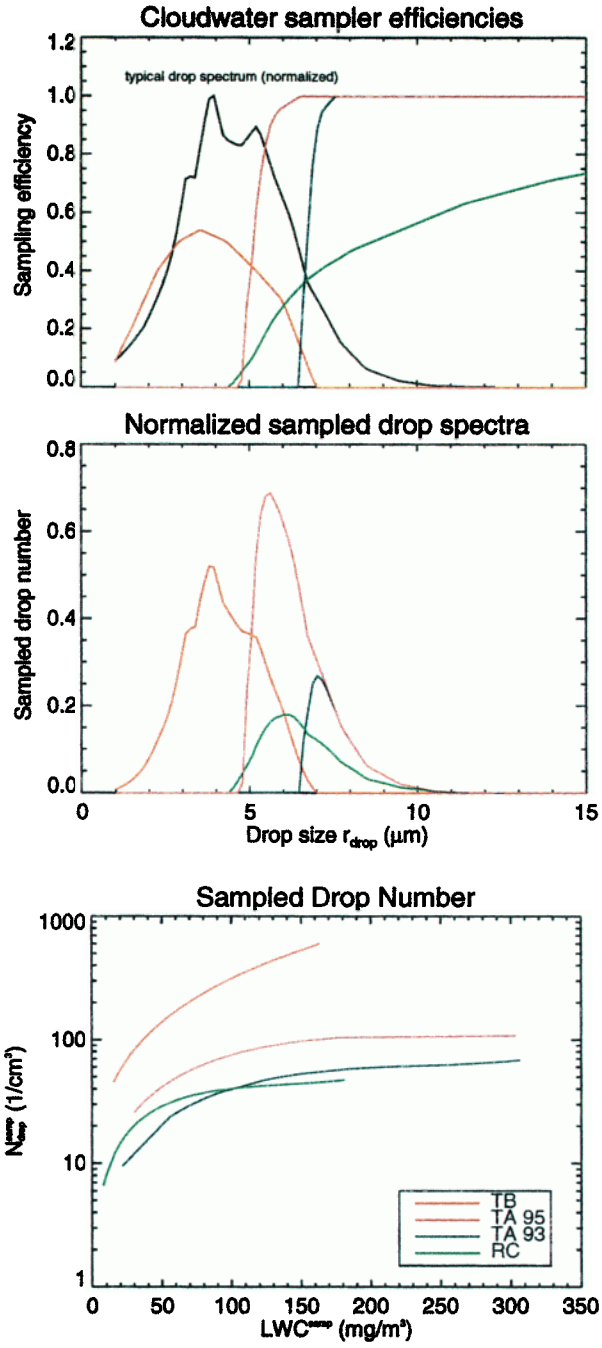

Plate 1. (top) Efficiency curves of the cloud water samplers (experimentally verified, for definition of colors see legend of bottom panel; black curve: normalized drop number $dN_d/d(\log r_d)$ of the typical weakly bimodal FSSP-cloud drop size spectrum). (middle) typical normalized sampled cloud drop size spectrum for each cloud water sampler (hourly average), calculated by superposing the FSSP-cloud spectrum with the efficiency curves of the samples $(dN_d/dt_d)_{FSSP} * Eff_{(TFI,RC)}$; see top panel. (bottom) Calibration curves relating the number of sampled drops (N_{drop}^{samp}) to the sampled liquid water content (LWC^{samp}), derived from 140 FSSP-drop spectra.

mation; (2) the mean number and size of sampled drops are determined from the sampled water mass by means of calibration functions ($N_{drop}^{samp}, r_{drop} = f(LWC^{samp})$); (3) the mean ion composition of cloud water (expressed by $\bar{\Lambda}_m$) does not vary to a great extent; and (4) no outgassing occurs during drop evaporation ($M_{sol}^{cloud} = AP_{sol}^{cp}$; see Table 5).

In the corresponding sections the validity of each statement for the continental measuring site Mount Kleiner Feldberg will be shown. We believe that the results achieved with the new method can be regarded as general for continental air masses because continental air is not influenced by strong local sources and away from coasts and therefore afford the necessary stability of the four key parameters. However, to transfer the method to other measuring sites, it is required primarily to determine these four basic pieces of informations, even at continental sites. For other sites, closer to or farther away from local sources, where the variability of aerosol soluble fraction, cloud drop distribution, composition of cloud water, and therefore outgassing may vary to a greater extent, it cannot be guaranteed that the method is applicable. The minimum number of measurements to consolidate the key statements is about 20 for the mean soluble fraction of aerosol particles and 100 for the calibration functions of the cloud drop spectra and the mean ion composition of cloud water. The statement on outgassing results from the other measurements.

2.1. Experiments and Instrumentation

During three extensive ground-based experiments at Mount Kleiner Feldberg, Germany (30 km west of Frankfurt/Main, 825 m above sea level (asl)) in November 1990, 1993, and 1995 (FELDEX 95), the following measurements were carried out:

2.1.1. Aerosol particles. Aerosol particles were sampled in 1993 and 1995 in cloud-free air before, in between, and after cloud occurrence and analyzed for their water-soluble and insoluble fraction using the measuring system SoFA (soluble fraction of aerosols – analyzer) [*Eichel et al.*, 1996], see section 2.2.1).

2.1.2. Cloud drop size spectra. Size spectra of the cloud drops were measured in 1995 simultaneously to the sampling of cloud water using a forward scattering spectrometer probe. From these measurements, a calibration curve is derived for each cloud water sampler relating the number and size of sampled drops N_{drop}^{samp}, r_{drop} to the sampled liquid water mass LWC^{samp} (see section 2.3).

Analysis of all measured cloud drop spectra yields that the typical microphysical structure of the clouds at Mount Kleiner Feldberg is weakly bimodal (see Plate 1, top, black curve) as also reported by *Arends et al.* [1994]. The peak in number density of mode 1 of the spectrum is found at drop sizes between 3 and 5 μm, whereas in mode 2, the peak of the drop number is located between 5 and 10 μm radius, depending on the CCN spectrum, supersaturation history, and the meteorological situation. Cloud drops in this size range have grown only by condensation and not by collision-coalescence. Though the peaks of the two modes are only weakly pronounced, we will distinguish between them throughout this paper, because the results are different for each mode (see sections 3.1 and 3.2). They should be interpreted as differing primarily in drop size and secondarily in number density.

2.1.3. Bulk cloud water. Cloud water was sampled in different drop size intervals during cloudy periods using different cloud water samplers. During November 1990, cloud drops were sampled hourly using a rotating arm collector (RC)($r_d >$ 7 μm, r_d: drop radius), a wide stream impactor especially applicable for the sampling of large drops [*Krämer and Schütz*, 1994]. In November 1993 and November 1995 cloud water samples were taken in three size classes using the RC and in addition the two-stage fog water impactor (TFI) [*Schell et al.*,

Table 2. Uncertainties and Errors, %

Parameter	Unit	Instrument					Meaning/Derivation
		SoFA	TB	TA93	TA95	RC	
1: ΔAP_{sol}	%	5					variation in time
2: ΔAP_{ins}	%	5					variation in time
3: ΔLWC^{samp}	mg/m^3		20	30	40	30	scatter around calibration functions
4: ΔN_{drop}^{samp}	cm^{-3}		22	20	30	19	$f(3)$, mean of all cloudwater samples
Δr_{drop}	μm		30	36	50	35	$f(3,4)$
5: $\Delta \bar{\Lambda}_m$	$\frac{\mu Scm^{-1}}{mgL^{-1}}$		9	9	9	9	mean variation of all cloudwater samples 1995
6: ΔH^+	$\mu eq/L$		5	5	5	5	mean meas. error of all cloudwater samples
7: $\Delta\sigma$	$\mu S/cm$		2	2	2	2	mean meas. error of all cloudwater samples
8: ΔC_{sol}	mg/L		10	10	10	10	$f(5, 6, 7)$
9: ΔC_{ins}	mg/L		11	8	9	9	mean meas. error of all cloudwater samples
ΔC_{tot}	mg/L		15	13	14	14	$f(8, 9)$
ΔC_{gas}	mg/L		17	15	15	15	$f(1, 2, 8, 9)$
ΔC_{ap}	mg/L		23	20	20	20	$f(1, 2, 8, 9)$
ΔM_{tot}	ng/drop		27	23	33	23	$f(1, 2, 4, 8, 9)$
ΔM_{gas}	ng/drop		28	25	33	24	$f(1, 2, 4, 8, 9)$
ΔM_{ap}	ng/drop		32	28	36	28	$f(1, 2, 4, 8, 9)$
ΔM_{ap}^{gas}	—		43	38	49	37	$f(1, 2, 4, 8, 9)$
Δr_{ap}	μm		32	28	36	28	$f(1, 2, 4, 8, 9)$
Δr_{cp}	μm		27	23	33	23	$f(1, 2, 4, 8, 9)$
Δgf	—		41	37	49	36	$f(1, 2, 4, 8, 9)$

For meaning of the symbols see Table 1.

1997]. The TFI is a double-stage jet impactor, sampling larger drops in the first stage (TA93, $r_d > 6.5$ μm, first version of the sampler; TA95, $r_d > 5$ μm, second version) and smaller drops in the second stage (TB, 2.5 μm $< r_d <$ 5 μm).

The efficiency curves of the cloud water samplers, which were all both theoretically calculated and experimentally verified, are shown in Plate 1 (top, green, RC; blue, TA93; magenta, TA95; red, TB). The cloud water samplers are designed to sample either in mode 1 or in mode 2 of the cloud drop spectrum. TB, the second stage of the TFI with the typical inversed v-shaped sampling characteristics of a double-stage impactor (see Plate 1, top, red curve), always samples small drops with a mean size of around 4–4.5 μm radius (Plate 1, middle, red curve). The mean sizes of cloud drops sampled from mode 2 with TA93, TA95, and RC range from 6.5 from 10.5 μm radius (Plate 1, middle, magenta, blue, and green curves). They are determined, on the one hand, by the efficiency curves of the respective sampler and, on the other hand, by the decreasing branch of the cloud drop spectrum (at larger drop radii). No drops with mean drop sizes from 4.5 to 6.5 μm radius can be sampled with these cloud water samplers (see, for example, Plate 2, top). To sample drops in this size range, the efficiencies of TFI(TA,TB) and RC would have to be shifted toward lower sizes. However, each sample would then contain a nonnegligible amount of drops from mode 1, which is less desirable than losing information on drops in the above mentioned size range. Here we have to note that this is the case in those samples taken with the sampler TA95 when the peak of mode 1 is close to 5 μm radius.

2.2. Soluble Fraction of Particles (AP_{sol})

The soluble fraction of aerosol particles in cloud-free air is one of the fundamental parameters used in the method (see Appendix). With the knowledge of the ratio AP_{sol}/AP_{ins} in aerosol particles in cloud-free air the cloud water mass concentration resulting from the gas scavenged by the cloud drops (C_{gas}) and the cloud water mass concentration originating from the activated particles (C_{ap}) are determined in this study. This ratio is measured as a constant value in particle size and time, which is shown in section 2.2.1. As mentioned in section 1, the calculation of C_{gas} and C_{ap} is only valid if the ratio AP_{sol}/AP_{ins} is also representative for that part of the particle spectrum which is activated during cloud formation. This crucial point for the data analysis is discussed in detail in section 2.2.2.

2.2.1. Mean soluble fraction of particles in cloud-free air: variation in particle size and time. The soluble fractions of particles in cloud-free air (AP_{sol}) were measured by the system SoFA [*Eichel et al.*, 1996; *Sprengard-Eichel et al.*, 1998] before, in between, and after different cloud events. SoFA analyzes the insoluble volume of single aerosol particles in six narrow size bands (mean radii 0.19, 0.28, 0.43, 0.64, 0.91, and 1.29 μm). The soluble fraction was then calculated using

$$AP_{sol} = 100 - AP_{ins}, \quad (1)$$

where 100 is the total particle volume in percent. The mean soluble fraction of particles measured at each particle size during the course of the experiment in 1995 (FELDEX) is shown in Table 3. The values are very stable in time and particle size, before, after, and in-between cloud occurrence. Deviations are not larger than 5% (see Table 2) during each experiment. The total average of AP_{sol} was found to be 65% in 1995 [*Sprengard-Eichel et al.*, 1998] and 59% in 1993 [*Eichel et al.*, 1996].

As also shown in Table 3, *Winkler* [1974], *Fuzzi et al.* [1988], and *Khlystov et al.* [1996] found the mean soluble fractions of continental aerosol particles to be 61, 64, and 64%, respectively. Obviously, variations of the mean soluble particle fraction are only small in continental air masses. As can be derived from *Sprengard-Eichel et al.* [1998], they are caused by the variation of both the number and the soluble fractions of the cloud-processed particles: they contribute, on average, 50% to the total number of particles (see Table 4) and their soluble fraction depends on the strength of the processing, which in

Table 3. Mean Soluble Fraction of Particles (AP_{sol}), Measured by SoFA at Six Sizes in the Range 0.19–1.29 μm radius, in Cloud-Free Air Before, in Between, and After Different Cloud Events

	Mean Soluble Fraction of Particles (AP_{sol}), %							
	Particle Radius, μm							
1995	0.19	0.28	0.43	0.64	0.91	1.29	Average[a]	Cloud Occurrence
Oct. 10	65.4	63.9	61.2	64.2	61.4	69.9	64.9	
Oct. 31	61.6	65.0	64.0		69.2	63.4	62.5	
Nov. 01								yes
Nov. 02								yes
Nov. 03								yes
Nov. 04			66.8					
Nov. 05	65.0			60.5			64.9	
Nov. 06	64.5	61.1	67.6	60.5			63.9	
Nov. 07								
Nov. 08								yes
Nov. 09								
Nov. 10		67.2	67.2			67.6	67.2	
Nov. 11	67.4							
Nov. 12	67.3	62.0				67.6	66.2	
						Total Average	65	Kleiner Feldberg, FRG, 1995
							59	Kleiner Feldberg, FRG, 1993
							61	Deuselbach, FRG, 1974[b]
							64	Po-Valley, Italy, 1988[c]
							64	The Netherlands, 1996[d]

[a]Averages are weighted by the number of particles in the different size intervals.
[b]*Winkler* [1974], $r_p > 0.3$ μm.
[c]*Fuzzi et al.* [1988], bulk filter samples.
[d]*Khlystov et al.* [1996], $r_p > 0.15$ μm.

turn results from the degree of pollution of the air mass with water-soluble trace gases.

Following the above arguments, we used for each experiment the total averages of AP_{sol}/AP_{ins} (see Table 3) as constants in our calculations. For 1990 the values from 1993 are taken because the strength of cloud processing was in the same range during these two experiments. In 1995 the cloud processing was stronger.

2.2.2. Mean soluble fraction of activated particles. As shown in the previous section, AP_{sol} is determined with SoFA as mean (bulk) value for particles with radii > 0.19 μm. However, the lowest size of the activated particles is found to be 0.035 μm radius at Kleiner Feldberg (see section 3.1). Here we will show that the mean value found by SoFA is also representative for those particles activated in a cloud.

Therefore the distribution of particle solubilities over the size spectrum has to be known. They are summarized for the Mount Kleiner Feldberg in Table 4 (top left part). It is found that in terms of particle solubility, the spectrum can be divided into two ranges, separated at about 0.05 μm radius. For smaller particles, two distinct particle types exist having soluble fractions of about 5 and 50% [*Svenningsson et al.*, 1994]. These two particle types are found at various measuring sites and can

Table 4. Mean Soluble Fraction (AP_{sol}) of Particles in Cloud-Free Air and Those Activated During Cloud Formation

	Cloud-Free Air		Cloud Water		
	Particle Radius, μm		Cloud Supersaturation, %		
Single Particles Soluble Fraction,[b] %	≤0.05[a]	>0.05[b]	0.15	0.2	0.3
	Number Frequency, %		Activation Radius, μm		
92	—	54	0.06	0.05	0.04
56	50	27	0.07	0.06	0.05
2	50	19	0.11	0.10	0.08
↓	Mean Soluble Fraction (AP_{sol}), %				
	Cloud-Free Air		Activated Particles		
Average[c] →	29.0	65.2	67.7	67.5	66.0

For a detailed discussion see section 2.2.2.
[a]Tandem-differential-mobility-analyzer (TDMA), 1990 [*Svenningsson et al.*, 1994].
[b]SoFA, 1995 [*Sprengard-Eichel et al.*, 1998] (SoFA measures in the size range ≥ 0.19 μm radius; for the range 0.05–0.19 μm the soluble fractions and number of frequencies are assumed to be the same, based on our measurements presented here and theoretical considerations [*Krämer*, 1998]).
[c]Averages are weighted by the number of particles in the different size intervals.

be regarded as ubiquitous [e.g., *Eichel et al.*, 1996]. For particles > 0.05 μm radius an additional third particle type, the cloud-processed particles, arises in the spectrum with a soluble fraction of about 90% [*Eichel et al.*, 1996; *Sprengard-Eichel et al.*, 1998; *Krämer*, 1998]; see also section 3.2 and Table 6), depending on the strength of cloud processing. The appearance of the cloud-processed particles at about 0.05 μm radius is as a consequence of the above mentioned lowest size of the activated particles being 0.035 μm.

The mean soluble fraction of particles in cloud-free air on Mount Kleiner Feldberg in 1995 is now calculated by averaging over the particle types and number frequencies shown in the top left-hand part of Table 4. Particles from 0.025 to 0.05 μm radius have a mean soluble fraction of 29%. For those in the radius range 0.05–1.0 μm, 65.2% soluble material is determined, which is nearly identical with the total average found by SoFA in 1995 (see Table 3) for particles > 0.19 μm. This is because the mean value of particle solubility is nearly constant for each particle size where cloud-processed particles exist (see also Table 3, measurements for different particle sizes).

Now the mean soluble fraction of those particles activated during cloud formation is calculated: Following Köhlers theory, particles are activated depending on their size and soluble fraction in the sense that a larger and/or more soluble particle is activated at smaller supersaturations than a smaller and/or less soluble particle. For a specific cloud supersaturation and soluble particle fraction a critical particle size exists controlling whether a particle is activated to a cloud drop or not. Only particles larger than this activation size are incorporated in the cloud.

In the top right-hand part of Table 4 the activation sizes of the three particle types, differing by their soluble fractions, are calculated for typical stratus cloud supersaturations using Köhlers theory. It is seen that for example, in a cloud with low supersaturation (0.15%) the nearly insoluble particles (5% soluble fraction) smaller than 0.11 μm radius are not activated, while all cloud-processed particles (90% soluble fraction) larger than 0.06 μm are incorporated into the cloud. Calculating now the mean soluble fraction of all activated particles leads to a slightly larger value (67.7%) than in cloud-free air, because of the lack of the nearly insoluble particles smaller than 0.11 μm radius. Raising the supersaturation to 0.2 or 0.3% lowers the activation sizes of all particle types. Subsequently, the mean soluble fractions again approach that in cloud-free air, because the insoluble particles smaller than 0.11 μm radius appear in the activated particle spectrum.

Summarizing, we state that the mean soluble fraction of particles measured with SoFA represents with good accuracy the mean soluble fraction of the activated particles and therefore can be used in our calculations.

2.3. Sampled Drop Number and Drop Size of a Bulk Cloud Water Sample

For the analysis presented below it is necessary to relate to each bulk cloud water sample the number of sampled drops ($N_{\text{drop}}^{\text{samp}}$) and their mean size ($r_{\text{drop}}$). Only with this piece of information is it possible to determine the desired parameters for cloud drops of a certain mean size from measurements in the bulk sample. To obtain $N_{\text{drop}}^{\text{samp}}$ and r_{drop}, functional relationships (defined as "calibration curves") are derived relating these parameters to the sampled bulk cloud water mass (via the liquid water content of the sampled drops LWC^{samp}, determined for TFI(TA,TB) and RC by dividing the sampled bulk cloud water mass by the sampled air volume).

The required calibration curves are derived from detailed measurements of cloud drop spectra (measured with an FSSP; see section 2.1) and the (experimentally verified) sampling efficiency curves of each cloud water collector (see Plate 1, top panel). For this purpose, the observed number size distribution of the cloud drops ($(dN_{\text{drop}}/dr_d)_{\text{FSSP}}$) are superposed with the efficiency curves of the cloud water collectors ($\text{Eff}(r_d)_{(\text{TFI,RC})}$) resulting in the sampled cloud drop spectra (see Plate 1, middle panel). The sampled cloud drop spectra can be regarded as a size band cut off from the total spectrum. For TB, this is due to its efficiency curve (double-stage impactor) and for TA93, TA95, and RC, the bands are determined, on the one hand, by the efficiency curves of the respective sampler and, on the other hand, by the decreasing branch of the cloud drop spectrum (see also section 2.1). This shape of the bands is the reason for the existence of the relations between the number $N_{\text{drop}}^{\text{samp}}$ as well as size r_{drop} of the sampled drops and their water mass LWC^{samp}.

Analysis of 140 measured FSSP-drop size spectra yields the desired functional relation for each cloud water sampler: For each individual FSSP-sample i, the number of drops sampled by the cloud water collector with the efficiency $\text{Eff}(r_d)$ is obtained by integration over the sampled drop spectrum:

$$N_{\text{drop},i}^{\text{samp}} = \int \left(\frac{dN_{\text{drop},i}}{dr_d} \cdot \text{Eff}(r_d) \right) dr_d, \tag{2}$$

where $dN_{\text{drop},i}$ is the total number of drops present in the cloud in the size interval dr_d. The sampled liquid water content $\text{LWC}_i^{\text{samp}}$, the desired parameter for the calibration, can then be calculated by summing up the masses of the sampled drops:

$$\text{LWC}_i^{\text{samp}} = \int \left(\frac{dM_{\text{drop},i}}{dr_d} \cdot \text{Eff}(r_d) \right) dr_d, \tag{3}$$

where $dM_{\text{drop},i} = \frac{4}{3}\pi\rho_w \, dN_{\text{drop},i}$ (ρ_w: density of water).

The calibration curves for each cloud water collector (TFI(TB,TA 93/95) and RC, see Plate 1, bottom)

$$N_{\text{drop}}^{\text{samp}} = f(LWC^{\text{samp}}) \tag{4}$$

are then derived by calculating the best fit through all FSSP—derived data pairs ($N_{\text{drop},i}^{\text{samp}}$, $\text{LWC}_i^{\text{samp}}$). With these functions, also the mean drop size of the sampled drops r_{drop} can be calculated

$$r_{\text{drop}} = \left(\frac{3}{4\pi} \cdot \frac{\text{LWC}^{\text{samp}}}{N_{\text{drop}}^{\text{samp}}} \right)^{1/3}. \tag{5}$$

Using these FSSP-derived calibration functions, $N_{\text{drop}}^{\text{samp}}$ and r_{drop} can now be calculated for the bulk cloud water samples taken with TFI(TA,TB) and RC only from the parameter LWC^{samp}. This procedure is applicable, when $\text{LWC}_{(\text{TFI,RC})}^{\text{samp}}$ (determined from TFI(TA,TB) or RC) is equal to $\text{LWC}_{(\text{FSSP})}^{\text{samp}}$ (derived from FSSP) to within the range of uncertainty of $\text{LWC}_{(\text{FSSP})}^{\text{samp}}$, which can be stated for our measurements. The uncertainties of the calibration functions and r_{drop} are listed in Table 2 and discussed in section 2.7.

2.4. Bulk Cloud-Water-Related Parameters (C_{sol}, C_{ins}, C_{ap}, C_{gas})

Following the overview in the Appendix, the analysis carried out for each bulk cloud water sample and the parameters

further calculated on the basis of these measurements are described in the subsequent sections.

2.4.1. Cloud water concentration of soluble mass (C_{sol}). The concentration of soluble mass in the bulk cloud water (C_{sol}) can be determined (using the method described by *Krämer et al.* [1996]) with good accuracy from the pH value and the electrical conductivity σ (measured immediately after sampling at 25°C under the assumption that no significant losses of soluble substances from cloud water have occurred prior to analysis; this is justified in section 2.6):

$$\rightarrow C_{sol} = \frac{\sigma - [H^+]\Lambda_{eqH^+}}{\bar{\Lambda}_m}, \quad (6)$$

where H^+ and $\Lambda_{eq_{H^+}} = 0.35\ \mu Scm^{-1}/\mu eqL^{-1}$ are the equivalent concentration and conductivity of the H^+ ions. $\bar{\Lambda}_m = 1.88\ \mu Scm^{-1}/mgL^{-1}$ is the mean mass conductivity of all other ions present in the cloud water, derived from the average composition at Mount Kleiner Feldberg. The average composition is determined from measurements of the anion and cation concentrations in cloud water sampled during a field experiment, simultaneous to our measurements, in 1990 [*Wobrock et al.*, 1994]. The uncertainty ΔC_{sol} is 10% and is mainly caused by the deviation of Λ_m from $\bar{\Lambda}_m$ in a single sample. Determination of Λ_m from detailed ion analysis for all samples from TFI(TA,TB) and RC 1995 shows that the mean deviation from $\bar{\Lambda}_m$ is only 9% (see Table 2). The small scattering of Λ_m demonstrates that it is very steady in cloud water and can therefore be used for each experiment at the Mount Kleiner Feldberg. This conclusion is supported by the same finding for rainwater: for eight rural and mountain-measuring sites $\bar{\Lambda}_m$, determined as annual average at each station, varies only by 3% around the total average of 1.93 $\mu Scm^{-1}/mgL^{-1}$ [*Krämer et al.*, 1996], which in turn is very close to the value found for cloud water.

2.4.2. Cloud water concentration of insoluble mass (C_{ins}). The concentration of insoluble mass (C_{ins}) is measured in each cloud water sample. It results from integration over the mass size spectrum of the insoluble particles in cloud water (stored at −18°C until the analysis), measured with a Coulter multisizer [*Krämer*, 1993; *Krämer and Schütz*, 1994] in the size range 0.3–10.0 μm radius:

$$\rightarrow C_{ins} = \int \left(\frac{dM_p}{dr_p}\right) dr_p, \quad (7)$$

where r_p and M_p are the size and the mass concentration of the insoluble particles. The mean uncertainties Δc_{ins}, caused by counting statistics and the width of the size interval dr_p range from 8 to 11% and are listed in Table 2 for TFI(TA,TB) and RC.

2.4.3. Cloud water mass concentration of scavenged particles and gases (C_{ap}, C_{gas}). As indicated in the Appendix, the mass concentration in the cloud water resulting from particle activation (C_{ap}) and gas scavenging (C_{gas}) can be calculated from the soluble and insoluble mass concentrations (C_{sol}, C_{ins}) in the cloud water and the relation of soluble to insoluble material in aerosol particles AP_{sol}/AP_{ins}.

The basic idea underlying this reasoning is that nucleation scavenging is the only pathway for insoluble mass to the liquid phase in the drop size range discussed here. An increase of mass by impaction scavenging of particles by cloud drops can be neglected [*Noone et al.*, 1992]. Therefore as long as no gas scavenging occurs, the ratio of soluble to insoluble material inside a drop (C_{sol}/C_{ins}) remains constant. Scavenging of atmospheric trace gases such as NH_3, SO_2, and HNO_3 and subsequent chemical reactions increase the soluble material

$$C_{sol} = C_{sol,ap} + C_{gas}, \quad (8)$$

where $C_{sol,ap}$ is the soluble mass originating from the activated particle. With this parameter the following equation holds during each stage of cloud lifetime

$$\frac{AP_{sol}}{AP_{ins}} = \frac{C_{sol,ap}}{C_{ins}}. \quad (9)$$

Introducing equation (8) in equation (9) leads to

$$\frac{AP_{sol}}{AP_{ins}} = \frac{C_{sol} - C_{gas}}{C_{ins}}. \quad (10)$$

Solving this equation for C_{gas} yields to a function of known parameters

$$\rightarrow C_{gas} = C_{sol} - \left(\frac{AP_{sol}}{AP_{in}} \cdot C_{ins}\right). \quad (11)$$

From the fact that the total mass concentration in cloud water can be calculated as sum of C_{ap} and C_{gas} ($C_{tot} = C_{ap} + C_{gas} = C_{sol} + C_{ins}$), C_{ap} can now be determined as

$$\rightarrow C_{ap} = C_{tot} - C_{gas}. \quad (12)$$

In a strict sense, these equations are only valid for a single particle nucleated to a drop in a cloud. For the application to bulk cloud water samples the mean (bulk) ratio of soluble to insoluble material in the aerosol particles AP_{sol}/AP_{ins} (1) has to be known with good accuracy and (2) must be representative for those particles activated to cloud drops. In section 2.2 it is shown, that these two, for the data analysis very important, points are satisfactorily fulfilled.

2.5. Cloud-Drop-Related Parameters (M_{ap}, M_{gas}, M_{ap}^{gas}, r_{ap})

With the knowledge of the FSSP-derived calibration functions (4) and (5) (see Appendix and section 2.3), the concentrations in the bulk cloud water samples can now be related to drops of a certain mean size for each cloud water sample.

2.5.1. Mean mass per drop of scavenged particles and gases (M_{ap}, M_{gas}, M_{ap}^{gas}). The mean mass of activated particles per drop (M_{ap}) and the mean mass of water-soluble trace gases entering a drop via gas scavenging (M_{gas}) can be determined for each sample using

$$\rightarrow M_{ap}(r_{drop}) = C_{ap}/N_{drop}^{samp}, \quad (13)$$

$$\rightarrow M_{gas}(r_{drop}) = C_{gas}/N_{drop}^{samp}. \quad (14)$$

Subsequently, the ratio of scavenged gas/particle mass per drop, defined as scavenging ratio, is

$$\rightarrow M_{ap}^{gas}(r_{drop}) = \frac{M_{gas}}{M_{ap}}. \quad (15)$$

2.5.2. Mean size of activated particles (r_{ap}). Knowing M_{ap}, the mean dry size of the activated particles (r_{ap}) can now be calculated using

$$\rightarrow r_{ap}(r_{drop}) = \left(\frac{3}{4\pi\rho_{ap}} M_{ap}\right)^{1/3}, \quad (16)$$

where the mean particle density ρ_{ap} is assumed to be 1.5 g/cm^3.

Table 5. Mean Soluble Mass Fraction in Cloud Water and in Processed Particles in Cloud-Free Air

	Mean Soluble Fraction, %			
	Cloud Water, M_{sol}^{cloud}			Processed Particles AP_{sol}^{cp}
	TB	TA	RC	SoFA
1993	89	90	88	88[a]
1995	95	95	93	92[b]

[a] *Eichel et al.* [1996].
[b] *Sprengard-Eichel et al.* [1998].

Cloud water and processed particles are sampled and analyzed independently but during the same experiments at Mount Kleiner Feldberg, Germany, before, in between, and after cloud events.

The similarity of the fractions of soluble material in cloud drops of different sizes to that of processed particles in cloud-free air ($M_{sol}^{cloud} = AP_{sol}^{cp}$) demonstrates that outgassing of water-soluble trace gases during evaporation of cloud drops and simultaneous formation of processed particles can here nearly be neglected.

2.6. Processed Particles (r_{cp}, gf)

Under the assumption, discussed below, that no outgassing occurs during drop evaporation, the parameters in drops can be transferred to the particles emerging during cloud dissipation.

2.6.1. Mean size of processed particles (r_{cp}). From the total mass $M_{tot} = M_{ap} + M_{gas}$, the mean size of processed particles r_{cp} is derived

$$\rightarrow r_{cp}(r_{drop}) = \left(\frac{3}{4\pi\rho_{ap}} M_{tot}\right)^{1/3}. \quad (17)$$

2.6.2. Mean growth factor (gf) of activated particles. The growth factor of a particle cycling through a cloud drop of a certain size is defined as

$$\rightarrow \mathrm{gf}(r_{drop}) = \frac{r_{cp}}{r_{ap}}. \quad (18)$$

2.6.3. Outgassing. Outgassing (escape of water-soluble gas when a cloud drop evaporates) occurs when the equilibrium between concentrations of water-soluble substances in the liquid and in the gas phase are distorted, i.e., if the atmosphere is clean in relation to the drop during evaporation. The higher the concentrations of water-soluble trace gases (especially HNO_3) in the atmosphere during evaporation the more soluble the material will remain in the drops [*Bower et al.*, 1997].

If outgassing would not occur, the soluble fraction of the resulting processed particles would be the same as that in the precursor drops ($AP_{sol}^{cp} = M_{sol}^{cloud}$). Under this condition the size and chemical composition of the cloud-processed particles can be determined from cloud water measurements.

To demonstrate that outgassing does not play an important role for our samples, we compare in Table 5 the mean soluble mass fraction in cloud water M_{sol}^{cloud}, sampled with TFI(TA,TB) and RC in 1993 and 1995, with that of cloud-processed particles AP_{sol}^{cp}, sampled and analyzed independently, but during the same experiments in cloud-free air with the system SoFA [*Eichel et al.*, 1996; *Sprengard-Eichel et al.*, 1998]. The values of AP_{sol}^{cp} are very stable in time and particle size, before, after, and in-between cloud occurrence, as already shown for the mean soluble fraction AP_{sol} of all particles (see section 2.2.1 and Table 3).

It is seen that for the smaller drops sampled with TA and TB the soluble mass fraction in cloud water is only slightly larger than in the processed particles in cloud-free air, while for the large drops sampled with RC, both values are identical. We assume that this is because the concentrations of soluble substances are higher in smaller drops. Altogether, outgassing can practically be neglected under the atmospheric conditions present during the field experiments.

2.7. Uncertainties and Errors

With the above described method we are able to determine parameters about aerosol processing in cloud drops, which until now could not be measured directly. The aim of this study is to determine these parameters for the first time experimentally. In spite of relatively large uncertainties (see below) the accuracy of the data is sufficient for an improved understanding of the mechanism of cloud processing.

In Table 2 the estimated uncertainties of all parameters are listed for each of the cloud water samplers. The first group of parameters is labeled with a number and represents the basic, directly measured inputs of the method. For a discussion of their errors see the respective sections (except of ΔLWC^{samp} and ΔN_{drop}^{samp}, which are discussed here). The errors of the further calculated parameters are derived from Gaussian error propagation; the errors upon which they depend are listed for each parameter.

The large uncertainties of the drop-related parameters (r_{drop}, M_{tot}, M_{gas}, M_{ap}, M_{ap}^{gas}, r_{ap}) and those related to the processed particles (r_{cp}, gf) are caused by the large uncertainties of the FSSP-derived calibration functions $N_{drop}^{samp} = f(LWC^{samp})$ (in particular regarding TA95, where the efficiency curve is not sufficiently adjusted to the drop number size spectrum (see section 2.1), which increases the uncertainty of the calibration function).

The uncertainties of N_{drop}^{samp} represent the scatter around each calibration function and include errors in the FSSP measurements in the size or the number of drops, uncertainties caused by the use of an hourly average of the drop spectra, etc. In this study we had to use these calibration functions because FSSP measurements were not available for all times when cloud water was sampled. In future studies the accuracy of the parameters related to drops and processed particles may be improved by recording FSSP-drop spectra simultaneously with cloud water sampling and then using $N_{drop,i}^{samp}$ (sampled drop number of an individual FSSP sample i, calculated from $(dN_{drop}/dr_d)_{FSSP}$ and $\mathrm{Eff}(r_d)_{(TFI,RC)}$ (see section 2.3, equation (2)) for their calculation.

A further source of uncertainty is the already mentioned low resolution in time (1 hour) of the measurements. Possibly, physical and chemical mechanisms in cloud processing faster than this time step become suppressed in the data. However, the minimum sampling time of the bulk cloud water is limited by the current state of development of the sampling and analyzing techniques. For future studies in this field it would be highly desirable to develop instrumentation providing a better time resolution. Moreover, it will be important to obtain a more comprehensive data set (e.g., continuous FSSP measurements). Nevertheless, the measurements show that several new and interesting pieces of information contained in the samples are not blurred by errors and uncertainties.

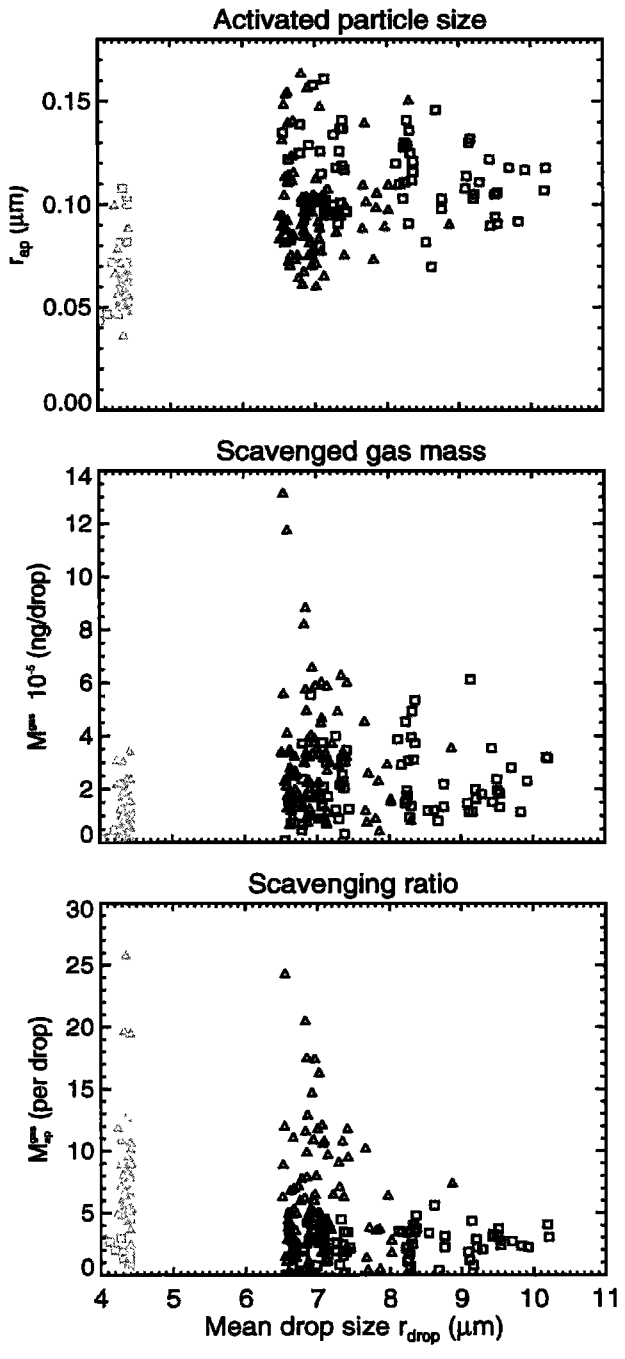

Plate 2. (top) Mean size of activated particles r_{ap}, (middle) scavenged gas mass M_{gas}, (bottom) scavenging ratio M^{gas}_{ap}, versus the mean drop size r_{drop} of modes 1 and 2 of the cloud drop spectra (for definition of the modes, see section 2.1; note that each observed stratus cloud is represented by several data points in modes 1 and 2, respectively).

3. Results

In this section the results achieved with the new method for continental particles cycling through stratus clouds during the field experiments on Mount Kleiner Feldberg/Ts., Germany, in 1990, 1993, and 1995 are presented. At first, the size-differentiated particle activation to drops of different size and the subsequent scavenging of trace gases in dependence on drop size is shown (section 3.1). With this information, the processing of different size particles in drops of various sizes is discussed (section 3.2). It should be called to mind here that the particle and droplet properties discussed in Plates 2 and 3 are derived from hourly sampled bulk cloud water. The data points do not represent a simultaneous measurement of a cloud drop or particle spectrum, but each point is a mean value from 1 hour sampling time.

3.1. Scavenging of Aerosol Particles and Gases by Cloud Drops

3.1.1. Activated particles. The size differentiated nucleation scavenging of aerosol particles by cloud drops is a func-

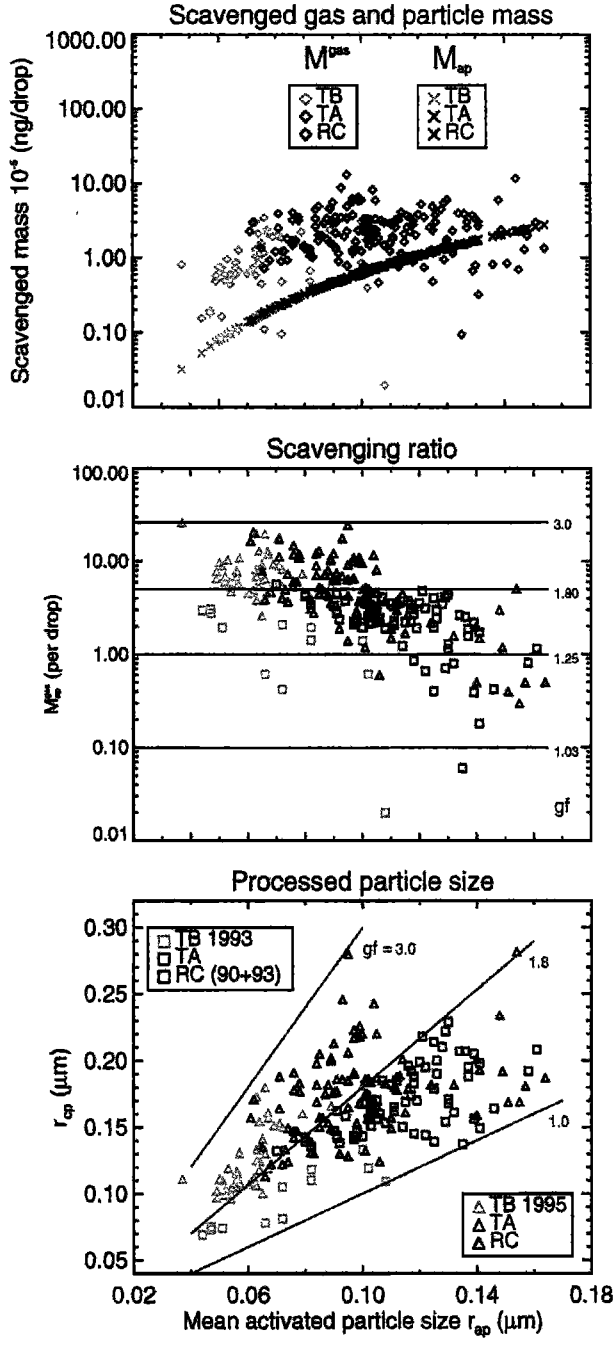

Plate 3. (top) Scavenged gas and particle mass M_{gas}, M_{ap}, (middle) scavenging ratio M^{gas}_{ap}, (bottom) size of the processed particles r_{cp} versus the mean size of activated particles r_{ap} (dark red lines: particles growth factor gf).

tion of the particle number size distribution and of their chemical composition as well as of the supersaturation at cloud formation and in the course of the lifetime of the cloud (see also section 2.2.2). The distribution of activated particles with sizes r_{ap} in cloud drops of different mean sizes r_{drop} is shown in Plate 2 (top) for all three field experiments. The lowest size of the activated particles is 0.035 μm radius, which is in good accordance with the results of *Svenningsson et al.* [1994] and *Hallberg et al.* [1994], who reported this value for Kleiner Feldberg in 1990 to be 0.03 μm and 0.035 μm, respectively. The agreement of the measurements is particularly remarkable when taking into account the completely different measuring methods: *Svenningsson et al.* [1994] compared aerosol size distributions in cloud-free air to interstitial particle size distributions in clouds, both measured with a differential mobility particle sizer; *Hallberg et al.* [1994] investigated cloud residual particles sampled with an impactor and analyzed using an electron microscope, while here the size of the activated particles is determined from the measurement of the soluble and insoluble mass in cloud drops (see section 2).

Another apparent structure in Plate 1 (top) is that in 1993 (open squares) the activated particles as well as the drops are, on average, larger than in 1995 (solid triangles), demonstrating the variability of aerosol particle size distributions and atmospheric conditions leading to a specific droplet population.

It is also seen in Plate 2 (top) that in the stratus clouds observed here the small drops of mode 1 of the drop spectra, represented by the measurements using TB (red symbols), have nucleated on smaller particles than the relatively large drops of mode 2 (TA, blue symbols and RC, green symbols; for definition of the modes see section 2.1; note here that each observed stratus cloud is represented by one data point in modes 1 and 2, respectively). The existence of a relationship between the size of activated particles and the mean size of sampled cloud drops was, near cloud base, also observed by *Heintzenberg et al.* [1989] in stratocumulus clouds. The finding that smaller droplets near cloud base have formed on smaller particles and larger drops on larger particles was further reported as a result of various earlier numerical studies by *Ogren and Charlson* [1992].

An explanation for this behavior can be derived from a recent model study of *Bott* [1997], who investigated in detail the diffusional growth of aerosol particles to stratiform cloud drops: In cases with high particle number densities in the cloud-forming air mass and therefore many activated particles, *Bott* [1997] found (after 6 hours of model time) that the growth of smaller particles to cloud drops is limited. They remain smaller than about 5 μm in radius in these scenarios because they stop growing if the supersaturation has become reduced by condensation. The larger particles grow further to larger drops having nearly the same mean sizes.

3.1.2. Scavenged trace gases. During cloud lifetime, various trace gases are scavenged by the drops. The amount of scavenged gas mass depends on many factors, such as, for example, the solubility of the gas, its gas phase concentration, the sizes of the drops, the concentrations inside the drops, and possible liquid phase reactions.

Even though several laboratory experiments [e.g., *Mitra et al.*, 1992; *Mitra and Hannemann*, 1993; *Hannemann et al.*, 1995] and various model studies [e.g., *Pandis et al.*, 1989; *Bott and Carmichael*, 1993; *Kulmala et al.*, 1993; *Wurzler et al.*, 1995; *Kulmala et al.*, 1998] examining the gas scavenging by drops have been carried out in recent years, no field measurements of the total amount of gas mass entering cloud drops of different sizes are reported in the literature.

Ogren and Charlson [1992] examined diagnostically the relative importance of the processes governing the solute mass in drops of different sizes. On the basis of theoretical arguments they predicted the solute mass to increase with drop size if the accumulation of solutes dominates the dilution of the drops by iffusive transfer of water to the drops (case 1). On the other hand, a decrease of solute mass with drop size is expected if the dilution of the drops dominates the accumulation of solutes (case 2).

The results of our measurements of the mass M_{gas} (per drop) of soluble trace gases entering cloud drops in the two modes are shown in Plate 2 (middle). The uptake of gas per drop is lower in the small drops of about 4.5 μm radius (red symbols) than in the smallest drops of the large drop mode (6.5–7.0 μm radius, green and blue symbols), implicating an accordance with the above described case 1 (solute mass increase with drop size) of *Ogren and Charlson* [1992] in this drop size range. This is true for both 1993 (open squares) and 1995 (solid triangles), where the uptake of trace gases exceeds strongly that in 1993. In contrast, for the entire drop mode 2, case 2 (solute mass decrease with drop size) of *Ogren and Charlson* [1992] is observed. The gas mass per drop reaches the highest values for clouds with smaller mean drop size and decreases when the mean drop size increases. This is especially true for the 1995 data and is less distinct in the data of 1993.

Such a different gas-scavenging behavior of the two drop modes is in accordance with the plausible growth history of these drop modes, described in the preceding section: It was supposed that the growth (i.e., dilution) of the small droplets is limited. This leads to a situation where the accumulation of solutes can dominate the dilution of drops and therefore M_{gas} increases with drop size (case 1 of *Ogren and Charlson* [1992], for the drop size range of about 4–7 μm radius). Furthermore, under the assumption that the larger drops of mode 2 grow further, dilution of the drops can dominate the accumulation of solutes and M_{gas} decreases with drop size (*Ogren and Charlsons* [1992] case 2, for the drop size range of about 7–10 μm radius).

3.2. Cloud Processing of Aerosol Particles

With the information from the previous section on the activation of particles to drops and the subsequent scavenging of trace gases, we can now discuss the modification of the activated particles when the cloud drops evaporate without outgassing (see section 2.6.3) and the activated particles are transferred to processed particles. The degree of modification (= processing) depends on the mass ratio of scavenged gas to the activated particles, defined as scavenging ratio (M_{ap}^{gas}) in section 2.5.1, in the sense that the processing increases with the scavenging ratio. In anthropogenically polluted regions the activated particles will be more strongly processed by clouds than in unpolluted regions because the concentration of trace gases in the gas phase, and therefore their uptake into cloud drops, is higher.

The order of magnitude of the scavenging ratio in the observed continental stratus clouds, is shown in Plate 2 (bottom). Although the mass of particles and gases is small in the small drops of mode 1 (see Plate 2, top and middle), the scavenging ratio M_{ap}^{gas} can reach values up to a factor of 25 in this drop mode, especially for the samples from 1995 where the gas uptake was high (see section 3.1.2). In the larger drops of mode 2, M_{ap}^{gas} decreases when the mean drop size increases and does not reach values as high as in mode 1. Values above 20 for M_{ap}^{gas}

are observed only for the sampler TA95, when the mean drop size is smaller than 7 μm radius. In these cases the samples probably also contain drops from mode 1 (see section 2.1). For 1993, where the gas uptake was low (see section 3.1.2), M_{ap}^{gas} shows no dependence on drop size but achieves values of between 0.02 and 5. Altogether, it can be concluded, that the strongest modification of the activated particles takes place in the smaller drops.

The scavenging ratio M_{ap}^{gas} is now related to the size r_{ap} of the activated particles (Plate 3, middle), the corresponding growth factors of the activated particles are marked in dark red in the plate. For illustration, M_{gas} and M_{ap} are also shown in dependence of r_{ap} in Plate 3 (top). It can be seen that in 1995 (solid triangles) the smallest activated particles are most strongly affected by cloud processing, which is in agreement with the model findings of *Bower and Choularton* [1993] and *Choularton et al.* [1996]. Particles smaller than about 0.1 μm can multiply their mass by a factor up to 25 while increasing their radii by up to a factor of 3. The larger particles grow to a maximum of 1.8 times their original size. The reason for this behavior is that the highest scavenging ratio M_{ap}^{gas} is found in the small drops containing the smallest particles (see Plate 2, top). For the data obtained in 1993 (open squares) we showed in the previous section that the gas uptake is much less than in 1995, especially for the small drops. Consequently, in 1993 the growth of the particles is not that strongly dependent on their original size. Particles of all observed sizes do not grow larger than slightly below twice (1.8) their initial size.

Nevertheless, even these values are large in comparison to those reported for marine air. *Kreidenweis et al.* [1996] investigated the chemical cloud processing as well as the cloud processing by collision-coalescence numerically and found a maximum growth factor of 1.25 in the stratocumulus-capped marine boundary layer. A growth factor of 1.2 is reported by *O'Dowd et al.* [1999] for marine stratocumulus, while maximum growth factors of about 2 are observed by *O'Dowd et al.* [1996] over the Pacific off the Californian coast. A plausible explanation for the difference between marine and continental air is that in a marine environment the concentrations of water-soluble trace gases are lower and therefore the processing is weaker.

The relationship between the size of the activated and the processed particles is shown in Plate 3 (bottom). Again, it is seen that growth factors above 1.8 are only reached by activated particles smaller than $\approx$0.1 μm radius (solid triangles, 1995). In addition, Plate 3 shows that particles in the size range 0.035–0.17 μm (activated particles) are transferred to the range 0.06–0.30 μm (processed particles) due to cloud cycling.

Recapitulating, we conclude that the degree of particle processing depends, on the one hand, on the amount of scavenged gas mass but is, mainly, inversely linked to the mass of the activated particles. For the activated particles the following situation applies: weak processing (scavenging ratio $M_{ap}^{gas} \leq 5$, growth factor gf $\leq$ 1.8; see Plate 3, middle) occurs at all observed particle sizes. Strong absolute mass gain (scavenging ratio $M_{ap}^{gas} > 5$, growth factor gf $>$ 1.8) is only observed for activated particles < 0.1 μm in radius. Activated particles with radii larger then 0.1 μm, mainly found in the larger drops of mode 2, will not be processed that strongly.

Therefore we conclude that the processing of these larger activated particles in larger cloud drops (mode 2) is of minor atmospheric impact because their radiative and nucleation properties do not change significantly. However, these larger drops transport water-soluble trace species from the gas to the liquid and finally to the particle phase.

The strongly processed small activated particles ($r_{ap} < 0.1$ μm), mostly found in the small drops of mode 1, are delivered as larger particles during cloud evaporation. The resultant processed particles possess significantly different direct and indirect radiative properties as well as nucleating properties because they have increased their size and soluble fraction in comparison to the activated particles. In the next cloud cycle, most of them will be found in the larger drops of mode 2. This finding is in accordance with *Bower et al.* [1997], who investigated numerically, constrained by field observations, the processing of particles by a hill cap cloud.

Thus we conclude that the processing of these small atmospheric particles in small cloud drops (mode 1) is, especially under polluted atmospheric conditions when high gas phase precursor concentrations lead to large concentrations of NO_3^-, $SO_4^=$, and NH_4^+ in the liquid phase, an important mechanism to convert particles from "little active" to "highly active" by raising both their size and hygroscopicity. It should be noted that the degree to which this transfer process occurs in the wet aerosol phase prior to cloud formation needs also to be considered and quantified. This is shown in model studies of *Korhonen et al.* [1996] and *Kulmala et al.* [1998] examining the uptake of trace gases during the growth of aerosol particles to cloud drops.

Altogether, this reasoning implies that the aerosol indirect and direct radiative forcing is influenced not only by the concentration and chemical composition of aerosol particles but also, to an unknown extent, by the gas phase concentrations of water-soluble trace gases such as HNO_3, NH_3, and SO_2. The cooling effect of aerosol particles on the Earth's climate can be intensified by increasing atmospheric amount of water-soluble trace gases and thus counteract the warming effect of the greenhouse gases.

4. Summary

In the present study, the cycling history of continental aerosol particles passing through cloud drops of different sizes is investigated experimentally, using a new method, during three field campaigns, performed on the Mount Kleiner Feldberg/Ts., Germany, in 1990, 1993, and 1995.

Our measurements show that the two drop modes of the observed stratus cloud drop size spectra differ in their microphysical and chemical behavior and, consequently, in particle processing. Moreover, two groups of activated particles are identified which are differently processed. These results are summarized in Table 6 and will now be briefly discussed:

On average, the particles activated in drop mode 1 are smaller than those incorporated in mode 2 (see Table 6, left). The model study by *Bott* [1997] shows that this phenomenon is found in stratus clouds forming in air masses containing high particle number densities. In this case the growth of smaller particles to drops is limited, the drops remain smaller than about 5 μm.

The mass of gas scavenged by the smaller drops of mode 1 is, on average, lower than that scavenged by the larger drops of mode 2. A possible explanation for this behavior can be derived from the diagnostic study of *Ogren and Charlson* [1992]: when the growth of drops is limited (like it is for the drops of mode 1), the gas mass scavenged by diffusive transfer is lower in smaller drops.

The processing of the activated particles (Table 6, middle) is stronger in drop mode 1 than in mode 2, because the scavenging ratio of gas to particle mass M_{ap}^{gas} reaches the highest values

Table 6. Minimum–Maximum Values in the Two Drop Modes, the Two Groups of Activated Particles and for Processed Particles

Drops				Activated Particles					Processed Particles
Drop Mode	r_{ap} μm	$M_{gas} \times 10^{-5}$ ng/drop	M_{ap}^{gas}	Particle Group	r_{ap} μm	M_{ap}^{gas}	gf	Drop Mode	r_{cp} μm
1	**0.035**	0.2	25	stongly	0.035	25	3	1	**0.06**
	0.11	3.5	0.02	processed	0.11	5	1.8		**0.3**
2	0.06	≈10	≈15	weakly	0.035	5	1.8	1 + 2	
	0.17	0.2	0.02	processed	0.17	0.02	1		

In the two drop modes: the size r_{ap} of the activated particles, the scavenged gas mass M_{gas}, and the scavenging ratio M_{ap}^{gas}; in the two groups of activated particles: r_{ap}, M_{ap}^{gas}, and the particle growth factor gf; processed particle size r_{cp} (mean drop size in drop mode 1: 3.0–5.0 μm; 2: 6.5–10.6 μm).

for the smaller drops. We observe two groups of activated particles: Strong processing occurs for particles belonging to the first group ($r_{ap} < 0.11$ μm, mostly found in the drops of mode 1), they can increase their size by factors between 1.8 and 3. Weaker processing is observed for the particles of the second group ($0.035 < r_{ap} < 0.17$ μm, found in drop mode 1 + 2), reaching a maximum of slightly below twice their original size. Altogether, the degree of particle processing depends on the amount of scavenged gas mass but is, mainly, inversely linked to the mass of the activated particles.

Consequently, the weaker processing of the larger activated particles ($r_{ap} \gtrsim 0.1$ μm) found in larger cloud drops (mode 2) is of lesser atmospheric impact because their radiative and nucleation properties do not change significantly.

The stronger processing of the smaller activated particles ($r_{ap} \lesssim 0.1$ μm radius) leads to a strong change in size and composition of the processed particles that would arise during cloud evaporation. These small activated particles, mostly found in the small drops of mode 1, have been converted to processed particles with significantly changed direct and indirect radiative as well as nucleation properties. This reasoning implies that the negative aerosol climate forcing is, to an unknown extent, intensified by water-soluble gas phase compounds such as HNO_3, NH_3, and SO_2.

Appendix: Overview of the Method

To make the method easier to understand, a summary of the measured and calculated parameters is given here. Parameters to be measured in each bulk cloud water sample of TFI (TA, TB) and RC are in braces in sections A2 and A3. The key statements central for the method are in quotes in sections A1, A2, A3, and A5.

A1. Measurements in Cloud-Free Air (see Section 2.2.2)

AP_{sol}/AP_{ins}, the mean soluble to insoluble fraction of aerosol particles, is measured using the instrument SoFA as a "constant value which is representative for activated particles."

A2. Measurements in Clouds (see Section 2.3)

$N_{drop}^{samp}, r_{drop} = f\{LWC^{samp}\}$, the number and size of sampled drops as a function of sampled liquid water mass, is "calculated from calibration functions."

The instrument used for calibration measurements is the FSSP, the instruments used to determine LWC^{samp} are the cloudwater samplers TFI(TA, TB) and RC.

A3. Measurements in Bulk Cloud Water in Different Drop Size Classes (see Section 2.4)

$C_{sol} = f\{pH, \sigma\}$, the soluble mass concentration, is "calculated by introducing a mean ion-composition of cloud water."

$\{C_{ins}\}$, the insoluble mass concentration, is measured using a Coulter Multisizer.

C_{gas}, the mass concentration from scavenged gas, and C_{ap}, the mass concentration from activated particles, are determined using AP_{sol}/AP_{ins} from A1.

Instruments used to sample bulk cloud water in different drop size classes are the cloud water samplers TFI(TA, TB) and RC (section 2.1).

A4. Measurements in Cloud Drops (see Section 2.5)

M_{gas}, the mass of scavenged gas per cloud drop, M_{ap}, r_{ap}, the mass and size of the activated particles, and M_{ap}^{gas}, the scavenging ratio of gas/particle mass, as well as the respective drop size r_{drop} are derived from the measurements in bulk cloud water (see section A3) using N_{drop}^{samp}, r_{drop} from section A2.

A5. Measurements in Processed Particles (see Section 2.6)

r_{cp}, the size of the processed particles, and gf, the growth factor of the activated particles, are determined from the measurements in cloud drops (see section A4), "under the assumption of no outgassing during drop evaporation."

Acknowledgments. The work is supported by the German Research Foundation through its *Sonderforschungsbereich 233* (SFB233): Chemistry and Dynamics of Hydrometeors. The field experiments in 1993 and 1995 (FELDEX 95) were organized in the frame of the SFB233 by the Institüt für Physik der Atmosphäre, Universitat Mainz, and the Zentrum fur Umweltforschung, Universität Frankfurt. The authors would like to thank all members of these institutes involved in the development and operation of the various instruments as well as those sampling and analyzing cloud water and aerosol samples under mostly inhospitable conditions. They also greatly acknowledge Keith Bower, Jutta Brinkmann, Daniel McKenna, and Rolf Müller for their support and stimulating scientific discussion.

References

Arends, B. G., et al., Microphysics of clouds at Kleiner Feldberg, *J. Atmos. Chem.*, *19*, 59–85, 1994.

Bott, A., The impact of the physico-chemical microstructure of atmospheric aerosols on the formation of stratiform clouds, *J. Aeros. Sci.*, *26*, S889–S890, 1995.

Bott, A., and G. R. Carmichael, Multiphase chemistry in a microphysical radiation fog model—A numerical study, *Atmos. Environ.*, *27*(A), 503–533, 1993.

Bott, A., T. Trautmann, and W. Zdunkowski, A numerical model of the cloud-topped planetary boundary layer: Radiation, turbulence and spectral microphysics in a marine stratus, *Q. J. R. Meteorol. Soc.*, *122*, 635–667, 1996.

Bott, A., A numerical model of the cloud-topped planetary boundary layer: Impact of aerosol particles on the radiative forcing of stratiform clouds, *Q. J. R. Meteorol. Soc.*, *123*, 631–656, 1997.

Bower, K. N., and T. W. Choularton, Cloud processing of the cloud

condensation nucleus spectrum and its climatological consequences, *Q. J. R. Meteorol. Soc.*, *119*, 655–679, 1993.

Bower, K. N., et al., Observations and modeling of the processing of aerosol by a hill cap cloud, *Atmos. Environ.*, *31*, 2527–2543, 1997.

Charlson, R. J., S. E. Schwartz, J. M. Hales, R. D. Cess, J. A. Coakley, Jr., J. E. Hansen, and D. J. Hofmann, Climate forcing by anthropogenic aerosols, *Science*, *255*, 423–430, 1992.

Choularton, T. W., et al., A study of the aerosol modification generated by passage through an orographic cloud, in *Proceedings of the 12th International Conference on Clouds and Precipitation*, *2*, 1145–1148, 1996.

Eichel, C., M. Krämer, L. Schutz, and S. Wurzler, The water-soluble fraction of atmospheric aerosol particles and its influence on cloud microphysics, *J. Geophys. Res.*, *101*, 29,499–29,510, 1996.

Fuzzi, S. (Ed.), The Kleiner Feldberg Cloud Experiment 1990, EUROTRAC subproject Ground-Based Cloud Experiment (GCE), *J. Atmos. Chem.*, *19*(1, 2), 1994.

Fuzzi, S. (Ed.), The Great Dun Fell Cloud Experiment 1993, EUROTRAC subproject Ground-Based Cloud Experiment (GCE), *Atmos. Environ.*, *31*(16), 1997.

Fuzzi, S., G. Orsi, G. Mardini, M. C. Facchini, M. Mariotti, S. McLaren, and E. McLaren, Heterogeneous processes in the Po Valley radiation fog, *J. Geophys. Res.*, *93*, 11,141–11,151, 1988.

Fuzzi, S., et al., Multiphase chemistry and acidity of clouds at Kleiner Feldberg, *J. Atmos. Chem.*, *19*, 87–106, 1994.

Hallberg, A., J. A. Ogren, K. J. Noone, K. Okada, J. Heintzenberg, and I. B. Svenningsson, The influence of aerosol particle composition on cloud droplet formation, *J. Atmos. Chem.*, *19*, 153–171, 1994.

Hallberg, A., K. J. Noone, and J. A. Ogren, Aerosol particles and clouds: Which particles form droplets?, *Tellus*, *Ser. B*, *50*, 59–75, 1998.

Hannemann, A. U., S. K. Mitra, and H. R. Pruppacher, On the scavenging of gaseous nitrogen compounds by large and small rain drops, I, A wind tunnel and theoretical study of the uptake and desorption of NH_3 in the presence of CO_2, *J. Atmos. Chem.*, *21*, 293–307, 1995.

Heintzenberg, J. (Ed.), The Po Valley Fog Experiment 1989, EUROTRAC subproject Ground-Based Cloud Experiment (GCE), *Tellus*, *Ser. B*, *44*(5), 1992.

Heintzenberg, J., J. A. Ogren, K. J. Noone, and L. Gardneus, The size distribution of submicrometer particles within and about stratocumulus cloud droplets on Mt. Åreskutan, Sweden, *Atmos. Res.*, *24*, 89–101, 1989.

Khlystov, A., G. P. A. Kos, H. M. Ten Brink, C. Kruisz, and A. Berner, Activation properties of ambient aerosol in The Netherlands, *Atmos. Environ.*, *30*, 3281–3290, 1996.

Korhonen, P., M. Kulmala, and T. Vesala, Model simulations of the amount of soluble mass during cloud droplet formation, *Atmos. Environ.*, *30*, 1773–1785, 1996.

Kramer, M., *Insoluble and Soluble Substances in Cloud Water* (in German), Reihe Physik, Verlag Shaker, Aachen, Germany, 1993.

Krämer, M., Alteration of atmospheric particle solubility by cloud processing, *J. Aerosol Sci.*, *29*, S3–S4, 1998.

Kramer, M., and L. Schutz, On the collection efficiency of a Rotating Arm Collector and its applicability to cloud—and fogwater sampling, *J. Aerosol. Sci.*, *25*, 137–148, 1994.

Krämer, M., M. Schüle, and L. Schütz, A method to determine rainwater solutes from pH and conductivity measurements, *Atmos. Environ.*, *30*, 3291–3300, 1996.

Kreidenweis, S. M., G. Feingold, B. Stevens, and W. R. Cotton, Cloud processing of aerosol in the stratocumulus-capped marine boundary layer, in *Proceedings of the 12th International Conference on Clouds and Precipitation*, *2*, 1161–1164, 1996.

Kulmala, M., A. Laaksonen, P. Korhonen, T. Vesala, and A. Ahonen, The effect of atmospheric nitric acid vapor on cloud condensation nucleous activation, *J. Geophys. Res.*, *98*, 949–958, 1993.

Kulmala, M., A. Toivonen, T. Mattila, and P. Korhonen, Variations of cloud droplet concentrations and the optical properties of clouds due to changing hygroscopicity: A model study, *J. Geophys. Res.*, *103*, 16,183–16,195, 1998.

Meischner, P. F., M. Hagen, T. Hauf, D. Heimann, H. Höller, U. Schuhmann, W. Jaeschke, W. Mauser, and H. R. Pruppacher, The field project CLEOPATRA, May–July 1992 in Southern Germany, *Bull. Am. Meteorol. Soc.*, *74*, 401–412, 1993.

Mitra, S. K., and A. Hannemann, On the scavenging of SO_2 by large and small rain drops, V, A wind tunnel and theoretical study of desorption of SO_2 from water drops containing S(IV), *J. Atmos. Chem.*, *16*, 201–218, 1993.

Mitra, S. K., A. Waltrop, A. Hannemann, A. Flossmann, and H. R. Pruppacher, A wind-tunnel and theoretical investigation to test various theories for the absorbtion of SO_2 by drops of pure water and water drops containing H_2O_2 and $(NH_4)_2SO_4$, in *Precipitation Scavenging and Atmosphere—Surface Exchange*, edited by S. E. Schwartz and W. G. N. Slinn, pp. 123–141, Hemisphere Publ. Corp., Washington, 1992.

Nemesure, S., R. Wagener, and S. E. Schwartz, Direct shortwave forcing of climate by the anthropogenic sulfate aerosol: Sensitivity to particle size, composition, and relative humidity, *J. Geophys. Res.*, *100*, 26,105–26,116, 1995.

Noone, K. J., et al., Changes in aerosol size- and phase distributions due to physical and chemical processes in fog, *Tellus*, *Ser. B*, *44*, 489–504, 1992.

O'Dowd, C. D., J. A. Lowe, and M. H. Smith, Observations and modelling studies of chemical cloud processing by marine stratocumulus, in *Proceedings of the 12th International Conference on Clouds and Precipitation*, *2*, 1172–1175, 1996.

O'Dowd, C. D., J. A. Lowe, and M. H. Smith, Observations and modelling studies of aerosol growth in marine stratocumulus—Case study, *Atmos. Environ.*, *33*, 3053–3062, 1999.

Ogren, J. A., and R. J. Charlson, Implications for models and measurements of chemical inhomogeneities among cloud droplets, *Tellus*, *Ser. B*, *44*, 208–225, 1992.

Pandis, S. N., J. H. Seinfeld, and C. Pilinis, Chemical composition differences in fog and cloud droplets of different sizes, *Atmos. Environ.*, *24*(A), 1957–1969, 1989.

Pilinis, C., S. N. Pandis, and J. H. Seinfeld, Sensitivity of direct climate forcing by atmospheric aerosols to aerosol size and composition, *J. Geophys. Res.*, *100*, 18,739–18,754, 1995.

Schell, D., et al., A two-stage impactor for fog droplet collection: Design and performance, *Atmos. Environ.*, *31*, 2671–2679, 1997a.

Schell, D., et al., The size dependent chemical composition of cloud droplets, *Atmos. Environ.*, *31*, 2561–2576, 1997b.

Schwartz, S. E., et al., Group report: Connections between aerosol properties and forcing of climate, in *Aerosol Forcing of Climate*, R. J. Charlson and J. Heintzenberg (Eds.), pp. 251–280, John Wiley, 1995.

Slingo, A., Sensitivity of the Earth's radiation budget to changes in low clouds, *Nature*, *343*, 49–51, 1990.

Sprengard-Eichel, C., M. Krämer, and L. Schütz, Soluble and insoluble fractions of urban, continental and marine aerosol, *J. Aerosol Sci.*, *29*, S175–S176, 1998.

Svenningsson, I. B., H. C. Hansson, A. Wiedensohler, K. J. Noone, J. Ogren, A. Hallberg, and R. Colvile, Hygroscopic growth of aerosol particles and its influence on nucleation scavenging in cloud: Experimental results from Kleiner Feldberg, *J. Atmos. Chem.*, *19*, 129–152, 1994.

Winkler, P., Die relative Zusammensetzung des atmosphärischen Aerosols in Stoffgruppen (The relative composition of atmospheric aerosol), *Meteorol. Rundsch.*, *27*, 129–136, 1974.

Wobrock, W., et al., The Kleiner Feldberg Cloud Experiment 1990, An overview, *J. Atmos. Chem.*, *19*, 3–35, 1994.

Wurzler, S., P. Respondek, A. I. Flossmann, and H. R. D. Pruppacher, Simulation of the dynamics, microstructure and aerosol particle scavenging of a precipitating and a nonprecipitating cloud by means of a detailed 2-D cloud model, *Betr. Phys. Atmos.*, *67*, 313–319, 1994.

Wurzler, S., A. I. Flossmann, H. R. Pruppacher, and S. E. Schwartz, The scavenging of nitrate by clouds and precipitation, I, A theoretical study of the uptake and redistribution of $NaNO_3$ particles and HNO_3 gas by growing cloud drops using an entraining air parcel model, *J. Atmos. Chem.*, *20*, 259–280, 1995.

Wurzler, S. C., Z. Levin, and T. G. Reisin, Cloud processing of dust particles and subsequent effects on drop size distributions, *J. Aeros. Sci.*, *28*, S427–S428, 1997.

M. Krämer, Institut für Stratospharische Chemie (ICG-1), Forschungszentrum Jülich, 52425 Jülich, Germany. (email: m.kraemer@fz-juelich.de)

N. Beltz, Zentrum für Umweltforschung, Universität Frankfurt, 60325 Frankfurt, Germany.

D. Schell, enviscope GmbH, Arnoldshainer Str. 5, 60489 Frankfurt/Main, Germany.

L. Schütz, C. Sprengard-Eichel, and S. Wurzler, Institut für Physik der Atmosphare, Universitat Mainz, 55099 Mainz, Germany.

(Received June 9, 1999; revised October 1, 1999;
accepted October 5, 1999.)